

Akzeptierter Artikel

Titel: Ground-State Structure of the Proton-Bound Formate Dimer by Cold-Ion Infrared Action Spectroscopy

Autoren: Daniel Thomas, Mateusz Marianski, Eike Mucha, Gerard Meijer, Mark A Johnson, and Gert von Helden

Dieser Beitrag wurde nach Begutachtung und Überarbeitung sofort als "akzeptierter Artikel" (Accepted Article; AA) publiziert und kann unter Angabe der unten stehenden Digitalobjekt-Identifizierungsnummer (DOI) zitiert werden. Die deutsche Übersetzung wird gemeinsam mit der endgültigen englischen Fassung erscheinen. Die endgültige englische Fassung (Version of Record) wird ehestmöglich nach dem Redigieren und einem Korrekturgang als Early-View-Beitrag erscheinen und kann sich naturgemäß von der AA-Fassung unterscheiden. Leser sollten daher die endgültige Fassung, sobald sie veröffentlicht ist, verwenden. Für die AA-Fassung trägt der Autor die alleinige Verantwortung.

Zitierweise: *Angew. Chem. Int. Ed.* 10.1002/anie.201805436
Angew. Chem. 10.1002/ange.201805436

Link zur VoR: <http://dx.doi.org/10.1002/anie.201805436>
<http://dx.doi.org/10.1002/ange.201805436>

Ground-State Structure of the Proton-Bound Formate Dimer by Cold-Ion Infrared Action Spectroscopy

Daniel A. Thomas,^[a] Mateusz Marianski,^[a] Eike Mucha,^[a] Gerard Meijer,^[a] Mark A. Johnson,^{*,[b]} and Gert von Helden^{*,[a]}

Abstract: The proton-bound dicarboxylate motif, $\text{RCOO}^- \cdot \text{H}^+ \cdot \text{OOCR}$, is a prevalent chemical configuration found in many condensed-phase systems. We study the archetypal proton-bound formate dimer, $\text{HCOO}^- \cdot \text{H}^+ \cdot \text{OOCH}$, utilizing cold-ion infrared action spectroscopy in the photon energy range of $400\text{--}1800\text{ cm}^{-1}$. The spectrum obtained at $\sim 0.4\text{ K}$ utilizing action spectroscopy of ions captured in helium nanodroplets is compared to that measured at $\sim 10\text{ K}$ by photodissociation of Ar-ion complexes. Similar band patterns are obtained by the two techniques that are consistent with calculations for a C_2 symmetry structure with a proton shared equally between the two formate moieties. Isotopic substitution experiments point to the nominal parallel stretch of the bridging proton appearing as a sharp, dominant feature near 600 cm^{-1} . Multidimensional anharmonic calculations, however, reveal that the bridging proton motion is strongly coupled to the flanking COO^- framework, an effect that is qualitatively in line with the expected change in $\text{C}=\text{O}$ bond rehybridization upon protonation.

The linkage formed when two neutral molecules or two anions are bound to a shared proton is a ubiquitous soft binding motif in condensed phase chemistry. Here we are concerned with the latter case, the simplest example of which is the classic FHF^- anion featuring a three-center, two electron bond,^[1] which accommodates the bridging proton at the midpoint of the heavy atoms. A more chemically significant anionic system involves the conjugate bases of carboxylic acids, $\text{RCOO}^- \cdot \text{H}^+ \cdot \text{OOCR}$. These complexes are commonly observed, for example, in the anhydrous deprotonation of acidic protons in ionic liquids.^[2] X-ray structures indicate that the two carboxylate groups binding the extra proton are equivalent, suggesting that, like FHF^- , the proton resides at the midway point between two oxygen atoms.^[3] Similarly, a recent report detailed a protein crystal structure exhibiting equivalent $\text{C}=\text{O}$ bond lengths in a proton-bound dicarboxylate motif, potentially indicating an equally shared proton.^[4] Because X-ray analysis does not reveal the location of the bridging proton, here we address its vibrational signature as well as those of the $\text{C}=\text{O}$ groups residing on the flanking anions to better understand the local mechanics of this linkage. We specifically focus on the isolated $\text{HCOO}^- \cdot \text{H}^+ \cdot \text{OOCH}$ anionic complex (hereafter denoted AHA^-) and analyze its vibrational spectrum obtained using two cryogenic ion spectroscopy

schemes, one involving capture and infrared photoexcitation in He droplets at 0.4 K ^[5] and the other based on photodissociation of the ions complexed with an Ar atom.^[6]

An interesting aspect of the AHA^- system is that proton attachment to one of the oxygen atoms in the carboxylate head group breaks the symmetry between the two equivalent $\text{C}=\text{O}$ groups in the carboxylate. This in turn suggests that proton accommodation by the pair of molecular anions requires an intramolecular structural deformation. Thus, in contrast to spectroscopic characterization of the proton-bound neutral complexes, AH^+A , which have relied exclusively on the character of the vibrations associated with the bridging proton,^[7] the carboxylates offer the opportunity to follow the evolution of the CO_2^- normal modes as the two CO_2^- groups deform to accommodate the bridging proton. This strategy has previously been applied to show that the intramolecular H-bond adopted by deprotonated dodecanedioic acid is, in fact, asymmetrical (i.e., with the proton closer to one oxygen atom at the vibrational zero-point level).^[8]

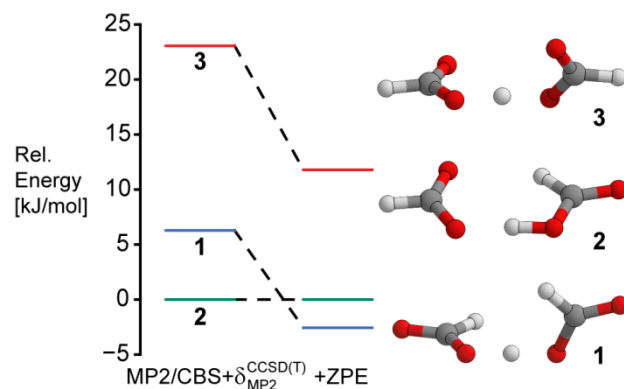


Figure 1. Relative energies, zero-point energy (ZPE) corrections, and structures of the three low-energy conformations of the protonated formate dimer, $\text{HCOO}^- \cdot \text{H}^+ \cdot \text{OOCH}$. Energies are derived from complete basis set (CBS) extrapolation^[9] from aug-cc-pVnZ ($n=3,4,5$)^[10] at the MP2 level of theory and corrected for the difference between MP2^[11] and CCSD(T)^[12] correlation energy in the aug-cc-pVTZ basis set.^[13] After inclusion of harmonic ZPE corrections, conformer 1 is predicted to be the most stable structure.

To anticipate the situation in the AHA^- system, Figure 1 presents three calculated low-energy structures, which illustrate the balance of forces that drive its structure. The lowest energy form 2, for example, features a largely electrostatic binding motif in which both the OH and CH groups orient themselves towards the negatively charged oxygen atoms on the carboxylate group, reminiscent of the “double contact” interaction reported earlier for the $\text{I}^- \cdot \text{HCO}_2\text{H}$ complex.^[14] The other two isomers, on the

[a] Dr. D. A. Thomas, Dr. M. Marianski, E. Mucha, Prof. Dr. G. Meijer, Prof. Dr. G. von Helden
Fritz-Haber-Institut der Max-Planck-Gesellschaft
Faradayweg 4–6, 14195 Berlin (Germany)
E-mail: helden@fhi-berlin.mpg.de

[b] Prof. Dr. M. A. Johnson
Sterling Chemistry Laboratory
Yale University
225 Prospect Street, New Haven, CT 06520 (USA)
E-mail: mark.johnson@yale.edu

Supporting information for this article is given via a link at the end of the document.

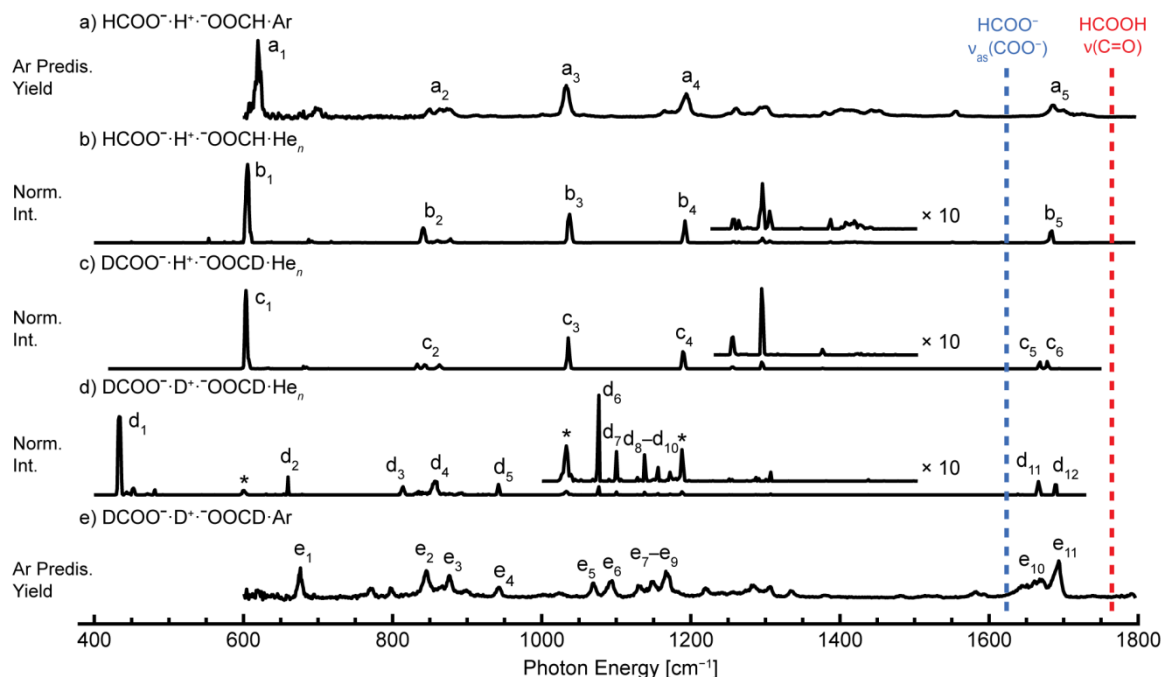


Figure 2. Vibrational spectra of the proton-bound dimer of formate, AHA^- , and its isotopically substituted variants by Ar predissociation spectroscopy and He nanodroplet ion spectroscopy. The blue and red lines mark the literature experimental values for formate $\nu_{\text{as}}(\text{COO}^-)^{[15]}$ and formic acid $\nu(\text{C}=\text{O})^{[16]}$ respectively. Strong agreement is observed between Ar tagging and He nanodroplet spectra for AHA^- (a, b) and the fully deuterated analogue, ADA^- (e, d). In the helium nanodroplet spectra, little change in the spectrum is observed upon deuterium substitution of the formyl hydrogens (c). In contrast, a demonstrable shift of the most intense transition from 605 cm^{-1} (b_1) to 433 cm^{-1} (d_1) is observed upon substitution of the shared proton. Features labeled with * in (d) result from proton back-exchange during ion trapping.

other hand, feature a bridging O–H–O motif in which the extra proton binds to one oxygen atom on each molecular anion. These structures differ according to the orientation of the organic scaffolds, with the higher-energy conformer **3** exhibiting opposing electric dipoles, and the lower-energy conformer **1** adopting an orientation in which the formate molecular dipoles are more favorably aligned. The delicate balance of forces underlying these structures is evident when one considers that the energy ordering of these isomers *changes* upon inclusion of the (harmonic) vibrational zero-point energies (ZPEs). Specifically, inclusion of harmonic ZPE corrections to the Born-Oppenheimer minima brings the more symmetrical, O–H–O isomer **1** below the double-contact structure **2**. Because these systems are widely recognized to be strongly anharmonic,^[7b, 7f, 17] we have undertaken the present experimental study to establish the structure adopted at 0.4 K in He droplets by analysis of its vibrational spectrum together with multidimensional anharmonic calculations. The temperature sensitivity of these conclusions is evaluated by extending the study to the warmer conditions afforded by the Ar “messenger tagging” technique.

Figures 2a and 2b show the vibrational spectrum of AHA^- collected between 400 and 1800 cm^{-1} utilizing the Ar tagging and helium nanodroplet techniques, respectively. In the spectrum obtained in helium nanodroplets, an intense spectral line is observed at 605 cm^{-1} , with other strong bands at 841, 1037, 1192, and 1684 cm^{-1} . The Ar tagging spectrum largely agrees with that measured in helium nanodroplets, with only minor shifts in frequency observed (Table S1). The relative intensities of weaker bands appear systematically reduced in the helium nanodroplet spectrum. This difference likely results from

the multiple-photon absorption process utilized to generate the action signal, which is expected to result in a nonlinear dependence of signal intensity on the transition strength for a given laser fluence.^[18]

As noted in the opening paragraphs, a straightforward differentiation of candidate AHA^- structures exhibiting either an equally shared (**1** and **3**) or localized proton (**2**) is given by the energies of the CO_2^- fundamentals. We focus here on the region of the carboxylate antisymmetric stretch, $\nu_{\text{as}}(\text{COO}^-)$, and the carboxylic acid C=O stretch, $\nu(\text{C}=\text{O})$. The red and blue lines in Figure 2 denote the experimental frequencies from the literature for formate $\nu_{\text{as}}(\text{COO}^-)$ and formic acid $\nu(\text{C}=\text{O})$,^[15-16] which serve as limiting cases for these features in the AHA^- spectrum. If the proton in AHA^- is localized on an oxygen atom, C=O stretching bands are expected to occur near $\nu_{\text{as}}(\text{COO}^-)$ and $\nu(\text{C}=\text{O})$, as predicted in the theoretical harmonic IR spectrum for the asymmetric conformer **2** (bands h_1 and h_2 , Figure 3d). However, in the experimental spectrum collected in helium nanodroplets, only a single feature is observed with maximum intensity at 1684 cm^{-1} (band b_5), close to the midpoint of the two limiting values expected for an asymmetric geometry. A broader band is found in the spectrum obtained by Ar predissociation spectroscopy (band a_5), however the prominent maxima are separated by less than 20 cm^{-1} , whereas separation of $\sim 100\text{ cm}^{-1}$ would be expected in the case of asymmetric proton localization.^[8, 19] In addition, fundamental harmonic transitions calculated for structure **1** predict two closely spaced bands in this region corresponding to in-phase and out-of-phase stretching of the two C=O bonds (band f_3 , Figure 3b), features that are possibly unresolved in the helium nanodroplet spectrum. Taken together, the CO_2^- normal modes observed experimentally are consistent

COMMUNICATION

WILEY-VCH

with the symmetric structure **1** for AHA^- in which the proton is shared equally between the carboxylate groups.

Further support for an equally shared proton is found in the intense features measured below 1200 cm^{-1} , which are likely associated with the vibrational modes of the shared proton.^[7a, 7b, 17, 20] However, assignment of the observed bands is not straightforward, as the highly anharmonic nature of the shared proton potential precludes harmonic vibrational analysis even for one-dimensional motion, and significant coupling between normal modes is also expected.^[7b, 20b, 21] Indeed, the theoretical harmonic IR spectra for conformers **1** and **2** fail to reproduce the low-frequency modes measured experimentally (Figures 3b, d). To assist in the assignments of the features in the lower energy range, we acquired the spectra of isotopically substituted variants of AHA^- . Both formyl hydrogen-deuterium substitution (Figure 2c) and carbon-13 substitution (Figure S1) were found to result in only minor changes in the spectra obtained in helium nanodroplets. In contrast, the spectrum of the fully deuterated dimer (ADA^-), in which the shared proton has been exchanged for a deuterium, differs significantly from that of the unlabeled species, as shown in Figure 2d. Most notably, a shift of the most intense spectral band from 605 cm^{-1} (b_1 , Figure 2b) to 433 cm^{-1} (d_1 , Figure 2d) is observed in the helium nanodroplet spectra. The spectrum of ADA^- measured with Ar tagging in the currently accessible photon energy range ($> 600\text{ cm}^{-1}$, Figure 2e) agrees well with that obtained by the helium nanodroplet method (Table S1).

The substantial H/D isotopic shift in the energy of band b_1 provides strong evidence that this feature is associated with displacement of the shared proton. In studies of other anionic proton-bound dimers, such intense spectral lines have been traced to the fundamental transition associated with proton motion parallel to the shared proton axis, ν_{\parallel} .^[17, 20a, 22] Interestingly, however, calculation of the frequency ratio between band b_1 of AHA^- and band d_1 of ADA^- yields a value of 1.40, which is inconsistent with the significantly larger frequency shift expected for an anharmonic potential well (e.g., a ratio of ~ 1.5 for deuterium substitution in a quartic potential).^[23] Thus, the vibrational mode associated with this band cannot be confidently assigned solely from the changes in band energies upon isotopic substitution.

To gauge the degree of coupling between the displacements of the shared proton and the deformations of the flanking HCOO^- ions, potential energy surfaces (PESs) of structure **1** in a normal coordinate basis were constructed and solved for their eigenstates and eigenvectors utilizing the discrete variable representation (DVR) method,^[20b, 24] as detailed in the Supporting Information. In the harmonic approximation, two intense bands below 1200 cm^{-1} are predicted by MP2 calculations for AHA^- (f_1 and f_2 , Figure 3b), corresponding to the fundamental of ν_{\parallel} and out-of-phase carboxylate deformation, $\delta(\text{OCO})_{\text{OOP}}$, respectively. However, utilizing one-dimensional (1D) PESs in the corresponding normal coordinate, the first excited states of ν_{\parallel} and $\delta(\text{OCO})_{\text{OOP}}$ are calculated to be nearly exactly isoenergetic, $\sim 899\text{ cm}^{-1}$ above the vibrational ground state (Table S2). Since both modes belong to the B symmetry species of the C_2 point group, the fundamental excitations couple strongly to yield mixed-character vibrational modes that can be represented as a linear combination of the contributing normal mode excited states on a two-dimensional (2D) PES (Figure S4). We find that the low-energy vibrational level (657 cm^{-1} above the ground state) is composed of 42% $\delta(\text{OCO})_{\text{OOP}}$ and 52% ν_{\parallel} first excited states, and the high-energy vibrational

level (1213 cm^{-1} above the ground state) is composed of 52% $\delta(\text{OCO})_{\text{OOP}}$ and 40% ν_{\parallel} first excited states. Higher excited states of $\delta(\text{OCO})_{\text{OOP}}$ and ν_{\parallel} contribute less than 5% to the coupled states (Table S3). These fractional contributions can also be applied to the Cartesian displacement vectors associated with the normal modes to evaluate the molecular motion for the coupled modes. Whereas normal modes ν_{\parallel} and $\delta(\text{OCO})_{\text{OOP}}$ both involve large-amplitude displacement of the shared proton along the O–H–O axis (Figure S5a, b), mode coupling largely confines shared proton motion to the high-energy coupled mode (Figure S5c), and carboxylate deformation is observed in the low-energy mode (Figure S5d). Animations of the coupled modes are available as Supporting Information.

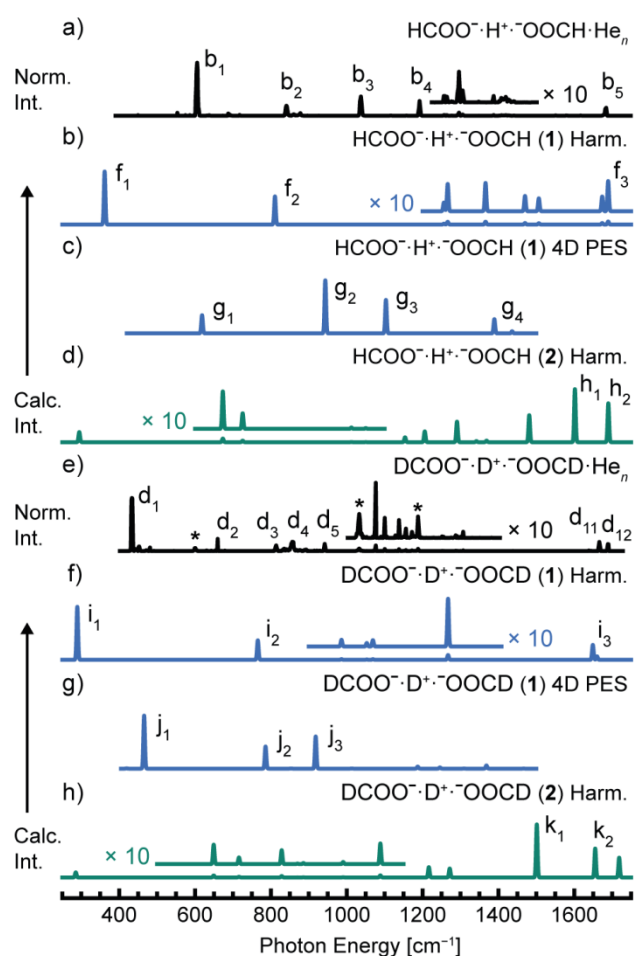


Figure 3. Experimental IR spectra of AHA^- (a) and ADA^- (e) compared to theoretical spectra. Spectra predicted in the harmonic approximation for conformers **1** (b, f) and **2** (d, h) at the MP2/def2-TZVPP level of theory (scaling factor 0.952) fail to replicate the intense features below 1200 cm^{-1} for both AHA^- and ADA^- . Theoretical spectra derived from a 4D PES for conformer **1** (c, g) show improved agreement with the experimental spectrum for both isotopologues, demonstrating the strong mode coupling in this system.

In ADA^- , the exchange of the shared proton for a deuterium leads to an energetic separation of the first excited states of ν_{\parallel} and $\delta(\text{OCO})_{\text{OOP}}$, which are calculated from 1D PESs to lie 595 cm^{-1} and 812 cm^{-1} above the ground state, respectively (Table S2). As a result, the vibrational levels remain largely decoupled in 2D PES calculations, with a low-energy level (544 cm^{-1} above the ground state) composed of 15% $\delta(\text{OCO})_{\text{OOP}}$ and 82% ν_{\parallel} and a high-energy level (891 cm^{-1} above the ground state)

COMMUNICATION

WILEY-VCH

composed of 83% $\delta(\text{OCO})_{\text{OOP}}$ and 15% ν_{\parallel} (Table S3). This result clearly demonstrates an isotope-dependent coupling of vibrational normal modes, providing a physical explanation for the smaller-than-expected frequency shift of band b_1 upon deuterium substitution.

Although strong coupling between ν_{\parallel} and $\delta(\text{OCO})_{\text{OOP}}$ is observed in the 2D PES for AHA^- , the predicted frequencies and intensities are insufficient to explain the bands observed experimentally (Table S2). To better account for coupling of proton motion to the intermolecular O–O distance, a four-dimensional (4D) PES was constructed for both AHA^- and ADA^- , adding the O–H–O symmetric stretch, $\nu_s(\text{O–H–O})$, and in-phase carboxylate deformation, $\delta(\text{OCO})_{\text{IP}}$, to the normal coordinate basis. Improved agreement in the predicted frequencies and intensities is observed utilizing this PES, with intense bands predicted for AHA^- at 619, 944, and 1103 cm^{-1} (bands g_1 , g_2 , and g_3 , Figure 3c) and for ADA^- at 466, 786, and 918 cm^{-1} (bands j_1 , j_2 , and j_3 , Figure 3g). A decomposition of the four-dimensional eigenvectors as a linear combination of normal mode eigenvectors shows significant contributions from states involving simultaneous excitation of multiple normal modes (i.e., combination bands, Tables S5, S6). We anticipate that more comprehensive multidimensional potential calculations, for example those that include formate torsional modes, will yield further insight into the origin of low-energy bands in the spectrum of AHA^- and ADA^- .

In summary, we have characterized the ground-state structure of the proton-bound formate dimer, $\text{HCOO}^- \cdot \text{H}^+ \cdot \text{OOCH}$, utilizing vibrational spectroscopy of ions trapped in helium nanodroplets and photodissociation of Ar-complexed ions. Analysis of the CO_2^- normal modes supports a symmetrical structure for the dimer with an equally shared proton. Preliminary multidimensional potential calculations reveal strong coupling between the vibrational normal modes and also show the strong isotope dependence of the mode coupling. It is intriguing to consider how the carboxylate substituent moiety may influence the structure and dynamics of proton-bound dimers, as the ground-state geometry and coupling of normal modes are likely highly sensitive to the identity of this functional group. Furthermore, knowing that the proton is localized in the intramolecular proton-bound dicarboxylate motif of deprotonated dodecanedioic acid,^[8] the question arises as to which structural constraints dictate the transition from shared to localized proton. These queries present appealing candidates for future studies to obtain a more comprehensive picture of the structure and dynamics of the prevalent proton-bound dicarboxylate motif.

Acknowledgements

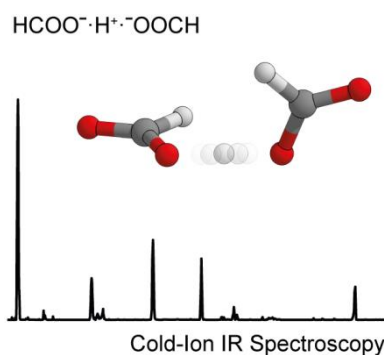
The authors thank Christopher Leavitt for acquisition of the Ar-tagging data and the FHI-FEL staff, particularly Sandy Gewinner and Wieland Schöllkopf, for laser operation. D.A.T. gratefully acknowledges the support of the Alexander von Humboldt Foundation. M.A.J. thanks the National Science Foundation under grant CHE-1465100.

Keywords: cold-ion spectroscopy • shared proton • coupling • carboxylate • helium nanodroplet

- [1] a) G. C. Pimentel, *J. Chem. Phys.* **1951**, *19*, 446-448; b) K. Kawaguchi, E. Hirota, *J. Chem. Phys.* **1986**, *84*, 2953-2960; c) K. Kawaguchi, E. Hirota, *J. Chem. Phys.* **1987**, *87*, 6838-6841; d) G. Pérez-Hernández, J. González-Vázquez, L. González, *J. Phys. Chem. A* **2012**, *116*, 11361-11369.
- [2] H. Rodríguez, G. Gurau, J. D. Holbrey, R. D. Rogers, *Chem. Comm.* **2011**, *47*, 3222-3224.
- [3] G. Gurau, H. Rodríguez, S. P. Kelley, P. Janiczek, R. S. Kalb, R. D. Rogers, *Angew. Chem., Int. Ed.* **2011**, *50*, 12024-12026.
- [4] J. Lin, E. Pozharski, M. A. Wilson, *Biochemistry* **2017**, *56*, 391-402.
- [5] a) A. I. González Flórez, E. Mucha, D.-S. Ahn, S. Gewinner, W. Schöllkopf, K. Pagel, G. von Helden, *Angew. Chem., Int. Ed.* **2016**, *55*, 3295-3299; b) E. Mucha, A. I. González Flórez, M. Marianski, D. A. Thomas, W. Hoffmann, W. B. Struwe, H. S. Hahn, S. Gewinner, W. Schöllkopf, P. H. Seeberger, G. von Helden, K. Pagel, *Angew. Chem., Int. Ed.* **2017**, *56*, 11248-11251.
- [6] A. B. Wolk, C. M. Leavitt, E. Garand, M. A. Johnson, *Acc. Chem. Res.* **2014**, *47*, 202-210.
- [7] a) K. R. Asmis, Y. Yang, G. Santambrogio, M. Brümmer, J. R. Roscioli, L. R. McCunn, M. A. Johnson, O. Kühn, *Angew. Chem., Int. Ed.* **2007**, *46*, 8691-8694; b) J. R. Roscioli, L. R. McCunn, M. A. Johnson, *Science* **2007**, *316*, 249-254; c) C. J. Johnson, A. B. Wolk, J. A. Fournier, E. N. Sullivan, G. H. Weddle, M. A. Johnson, *J. Chem. Phys.* **2014**, *140*, 221101; d) J. A. Fournier, C. T. Wolke, M. A. Johnson, T. T. Odbadrakh, K. D. Jordan, S. M. Kathmann, S. S. Xantheas, *J. Phys. Chem. A* **2015**, *119*, 9425-9440; e) C. T. Wolke, J. A. Fournier, L. C. Dzugan, M. R. Fagiani, T. T. Odbadrakh, H. Knorke, K. D. Jordan, A. B. McCoy, K. R. Asmis, M. A. Johnson, *Science* **2016**, *354*, 1131-1135; f) Y. Yang, O. Kühn, G. Santambrogio, D. J. Goebbert, K. R. Asmis, *J. Chem. Phys.* **2008**, *129*, 224302; g) D. T. Moore, J. Oomens, L. van der Meer, G. von Helden, G. Meijer, J. Valle, A. G. Marshall, J. R. Eyler, *ChemPhysChem* **2004**, *5*, 740-743.
- [8] M. Z. Kamrath, R. A. Relph, T. L. Guasco, C. M. Leavitt, M. A. Johnson, *Int. J. Mass Spectrom.* **2011**, *300*, 91-98.
- [9] A. Halkier, T. Helgaker, P. Jørgensen, W. Klopper, J. Olsen, *Chem. Phys. Lett.* **1999**, *302*, 437-446.
- [10] R. A. Kendall, T. H. Dunning, Jr., R. J. Harrison, *J. Chem. Phys.* **1992**, *96*, 6796-6806.
- [11] C. Møller, M. S. Plesset, *Phys. Rev.* **1934**, *46*, 618-622.
- [12] a) K. Raghavachari, G. W. Trucks, J. A. Pople, M. Head-Gordon, *Chem. Phys. Lett.* **1989**, *157*, 479-483; b) R. J. Bartlett, J. D. Watts, S. A. Kucharski, J. Noga, *Chem. Phys. Lett.* **1990**, *165*, 513-522.
- [13] M. O. Sinnokrot, E. F. Valeev, C. D. Sherrill, *J. Am. Chem. Soc.* **2002**, *124*, 10887-10893.
- [14] W. H. Robertson, J. A. Kelley, M. A. Johnson, *J. Chem. Phys.* **2000**, *113*, 7879-7884.
- [15] H. K. Gerardi, A. F. DeBlase, X. Su, K. D. Jordan, A. B. McCoy, M. A. Johnson, *J. Phys. Chem. Lett.* **2011**, *2*, 2437-2441.
- [16] I. D. Reva, A. M. Plokhotnichenko, E. D. Radchenko, G. G. Sheina, Y. P. Blagoi, *Spectrochim. Acta, Part A* **1994**, *50*, 1107-1111.
- [17] E. G. Diken, J. M. Headrick, J. R. Roscioli, J. C. Bopp, M. A. Johnson, A. B. McCoy, *J. Phys. Chem. A* **2005**, *109*, 1487-1490.
- [18] a) F. Filsinger, D.-S. Ahn, G. Meijer, G. von Helden, *Phys. Chem. Chem. Phys.* **2012**, *14*, 13370-13377; b) A. I. González Flórez, D.-S. Ahn, S. Gewinner, W. Schöllkopf, G. von Helden, *Phys. Chem. Chem. Phys.* **2015**, *17*, 21902-21911.
- [19] C. T. Wolke, A. F. DeBlase, C. M. Leavitt, A. B. McCoy, M. A. Johnson, *J. Phys. Chem. A* **2015**, *119*, 13018-13024.
- [20] a) N. Heine, T. I. Yacovitch, F. Schubert, C. Brieger, D. M. Neumark, K. R. Asmis, *J. Phys. Chem. A* **2014**, *118*, 7613-7622; b) J. A. Tan, J.-L. Kuo, *J. Phys. Chem. A* **2015**, *119*, 11320-11328.
- [21] L. R. McCunn, J. R. Roscioli, M. A. Johnson, A. B. McCoy, *J. Phys. Chem. B* **2008**, *112*, 321-327.
- [22] N. Heine, K. R. Asmis, *Int. Rev. Phys. Chem.* **2014**, *34*, 1-34.
- [23] R. P. Bell, *Proc. R. Soc. London, Ser. A* **1945**, *183*, 328-337.
- [24] a) D. T. Colbert, W. H. Miller, *J. Chem. Phys.* **1992**, *96*, 1982-1991; b) J. C. Light, T. Carrington, in *Advances in Chemical Physics*, John Wiley & Sons, Inc., **2007**, pp. 263-310.

COMMUNICATION

The proton-bound dicarboxylate motif, $\text{RCOO}^- \cdot \text{H}^+ \cdot \text{OOCR}$, is encountered frequently, for example in protic ionic liquids and protein active sites. However, the location of the bridging proton can be challenging to ascertain. Cold-ion IR spectroscopy reveals that the isolated formate proton-bound dimer, $\text{HCOO}^- \cdot \text{H}^+ \cdot \text{OOCH}$, exhibits a fully shared proton. Bridging proton motion is also found to couple strongly to deformation of the flanking $-\text{COO}^-$ framework.



Daniel A. Thomas, Mateusz Marianski, Eike Mucha, Gerard Meijer, Mark A. Johnson, and Gert von Helden**

Page No. – Page No.

Ground-State Structure of the Proton-Bound Formate Dimer by Cold-Ion Infrared Action Spectroscopy